NANO LETTERS

2008
Vol. 8, No. 1
253−259

Supramolecular Porphyrin Polymers in Solution and at the Solid–Liquid Interface

Richard van Hameren,[†] Arend M. van Buul,[†] Maria A. Castriciano,[‡] Valentina Villari,[§] Norberto Micali,[§] Peter Schön,[†] Sylvia Speller,[†] Luigi Monsù Scolaro,[‡] Alan E. Rowan,[†] Johannes A. A. W. Elemans,*[,†] and Roeland J. M. Nolte[†]

Institute for Molecules and Materials, Radboud University Nijmegen, Toernooiveld 1, 6525 ED Nijmegen, The Netherlands, Università di Messina, Dipartimento di Chimica Inorganica, Chimica Analitica e Chimica Fisica, Salita Sperone 31, 1-98166 Vill. S. Agata, Messina, Italy, CNR - Istituto per i Processi Chimico-Fisici, Salita Sperone Contrada Papardo, 98158, Messina, Italy

Received October 5, 2007; Revised Manuscript Received November 16, 2007

ABSTRACT

We have investigated in detail the self-assembly of a chiral porphyrin trimer in different solvents and correlated this behavior to the aggregation of the molecule at a solid–liquid interface. In *n*-hexane and cyclohexane, CD spectroscopy and dynamic and static light scattering studies showed that the porphyrin trimer self-assembles already at micromolar concentrations into long, chiral supramolecular polymers, which precipitate as fibers when the solution is drop-cast onto a mica surface. In contrast, in chloroform, the compound is molecularly dissolved up to concentrations of 0.2 mM and when micromolar solutions are drop-cast onto mica, no precipitation of large assemblies occurs. Instead, at the moment that the chloroform film becomes subject to spinodal dewetting and the porphyrin trimers within this film start to self-assemble, extended patterns of equidistant lines of single molecule thick columnar stacks are formed.

The construction of predetermined patterns on surfaces is one of the major challenges in developing new technological applications.[1−3] To date, however, only a few examples of complex patterned surfaces that do not require a lithography step are known, and these patterned surfaces are often of small spatial extent.[4−10] Recently, we have shown that it is possible to construct highly ordered patterned surfaces simply by placing a chloroform solution containing porphyrin trimer **1a** (Figure 1A) on a mica surface and allowing the chloroform to evaporate.[4] The patterns consist of equidistant single molecular stacks of **1a** and it was demonstrated that their size can be extended to several square millimeters. The patterns are formed as a result of a delicate balance between physical dewetting processes and highly directional supramolecular interactions. As a result of this so-called "coffee-stain mechanism", a local increase in the concentration of **1a** occurs near the contact-line of the evaporating droplet. Further evaporation leads to unpinning and retraction of the contact line and the deposition of **1a** onto the mica surface. The obtained highly uniform periodicity is attributed to the propensity of the molecules of **1a** to form columnar stacks in the separate process of spinodal dewetting, which causes an undulating pattern in a thin evaporating film.

Intuitively, it is expected that the presence of large aggregates in solution will result in the generation of large surface architectures at a solid−liquid interface, whereas monomers or smaller aggregates will lead to smaller surface architectures.[11] In the present study we have investigated in detail the aggregation behavior of porphyrin trimers in solution and have studied the crucial role of the solvent. In addition, the aggregation behavior of these molecules in solution will be correlated to their behavior at a solid−liquid interface.

Circular dichroism (CD) has been proven to be a powerful tool to obtain information about the precise self-assembly process of a chiral compound into an aggregated structure.[12−14] To study the self-assembly of the porphyrin trimers in more detail, we have replaced the *n*-alkyl tails of **1a** with chiral ones to give compound **1b** (Figure 1A). Because of its resemblance with **1a**, it can be expected that also **1b** will self-assemble in solution into helical columnar stacks as a result of hydrogen bonding and $\pi-\pi$ interactions (Figure 1B,C). In the case of **1b**, however, the chirality of the molecule is expected to induce single handedness into these stacks, which can be analyzed by CD.

* Corresponding author. E-mail: J.Elemans@science.ru.nl.
† Radboud University Nijmegen.
‡ Università di Messina.
§ CNR-IPCF.

10.1021/nl072563f CCC: $40.75
Published on Web 12/04/2007

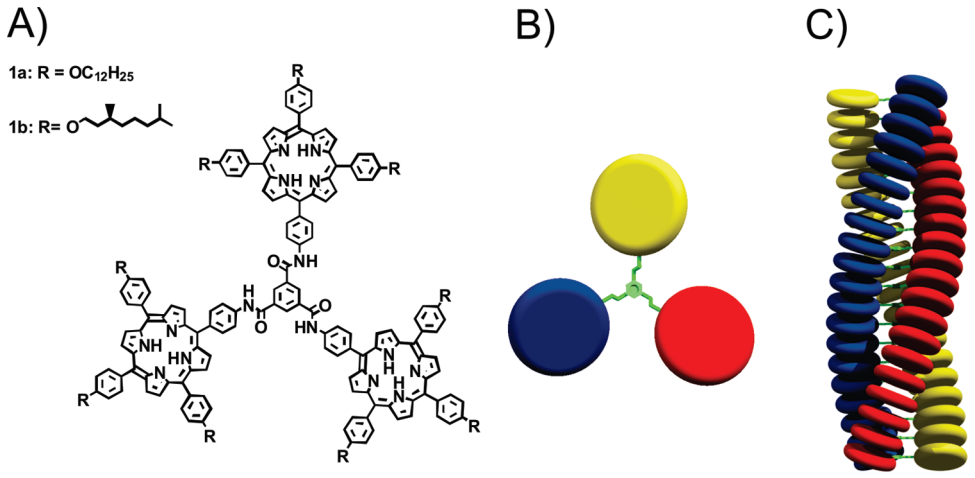

Figure 1. (A) Chemical structures of **1a** and **1b**. (B) Schematic representation of **1**. (C) Schematic representation of a self-assembled columnar stack of **1**.

Using *S*-(−)citronellol as the source of chirality, the synthesis of **1b** is straightforward (see Supporting Information). To study the aggregation behavior of **1b** in solution, it was decided to use chloroform, *n*-hexane and cyclohexane, because these solvents do not significantly interfere with hydrogen bonding and $\pi-\pi$ stacking interactions between the molecules. It is furthermore known that the use of these solvents can give rise to significant differences in aggregation behavior, because it has been shown that nonpolar alkanes poorly solvate the extended aromatic cores of self-assembling disklike molecules.[15,16]

The ^{1}H NMR spectrum of **1b** in $CDCl_3$ ([**1b**] = 2.3×10^{-3} M, Figure 2A) showed very broad signals, which indicates a strong aggregation of the compound in this solvent. The ^{1}H NMR spectrum became sharp after the addition of DMSO-d_6, which breaks up the hydrogen-bonding network and dissolves the aggregates of **1b**. Disassembly of the compound could also be achieved by diluting the sample. Because the ^{1}H NMR spectrum of **1b** sharpened up at concentrations below ~0.2 mM (Figure 2A), this concentration can be roughly considered as the critical aggregation concentration in this solvent. In contrast, in hexane-d_{14} the ^{1}H-spectra remained broad even at very low concentrations ([**1b**] = 1×10^{-5} M).

UV−vis measurements of **1b** in chloroform showed the presence of a relatively sharp Soret band at 423 nm ([**1b**] = 8.3×10^{-6} M, Figure 2B), indicating that this compound was molecularly dissolved. In contrast, the UV−vis spectrum of **1b** in *n*-hexane showed a broadened Soret band exhibiting absorption maxima at 403 and 422 nm and a shoulder at 439 nm, which is caused by excitonic coupling between neighboring porphyrin units. According to the exciton theory, a blue shift of the Soret band implies that the porphyrins are oriented face-to-face.[17,18] The UV−vis spectrum of **1b** in cyclohexane also showed a broadening and shifting of the Soret band. In this case two bands with maxima at 402 and 426 nm and an additional red-shifted band at 441 nm were observed, which suggests that in this solvent the porphyrins are oriented in both head-to-tail and face-to-face orientations. From the UV−vis data it is impossible to elucidate whether the stacking of the porphyrin moieties of **1b** is intra- or intermolecular, although from studies on similar molecules, the former is highly improbable.[4] When the absorbance of the bands at 403 and 423 nm was plotted as a function of concentration, in both cases Lambert−Beer behavior was observed (Figure 2C,D), indicating either intramolecular porphyrin stacking or the presence of very stable aggregates over the measured concentration range. Because molecular modeling calculations showed that intramolecular stacking between the porphyrin moieties within one molecule of **1b** is impossible,[4] it is proposed that in *n*-hexane **1b** forms aggregates already below micromolar concentrations. The large difference in UV-absorbance observed between two similar solvents, cyclohexane and *n*-hexane, highlights the important role of the solvent shell in defining the helical stacking. This first shell can be considered to be more like a "solvent−helix complex".

To investigate whether **1b** aggregates into helical columnar stacks, the chirality of the compound was used as probing tool. In chloroform, a solvent in which **1b** is molecularly dissolved at low concentrations ([**1b**] = 8.3×10^{-6} M), no CD effect was observed. In *n*-hexane, the CD spectrum clearly indicated the presence of chiral assemblies (Figure 3A). The complicated spectrum is the result of a mixture of three Cotton effects centered at 402, 426, and 438 nm, respectively (see Supporting Information), which can be correlated to the above-mentioned absorption bands in the UV−vis spectrum. These Cotton effects turned out to be temperature dependent (Figure 3B): upon an increase in the temperature from 30 to 42 °C, several changes, which were reversible upon cooling, were observed in the CD spectrum. Upon heating, the Cotton effect located at 403 nm slightly decreased and the Cotton effects at 426 and 438 nm changed sign; the latter increased in magnitude at the expense of the Cotton effect at 403 nm. The reversible changes in the spectra resulted in three isodichroic points located at 399, 425, and 438 nm, indicating a transition between two well-defined species. Upon an increase in temperature, the UV−vis spectrum showed an increase in the absorbance at 438 nm and a decrease in the absorbance at 403 and 422 nm, with

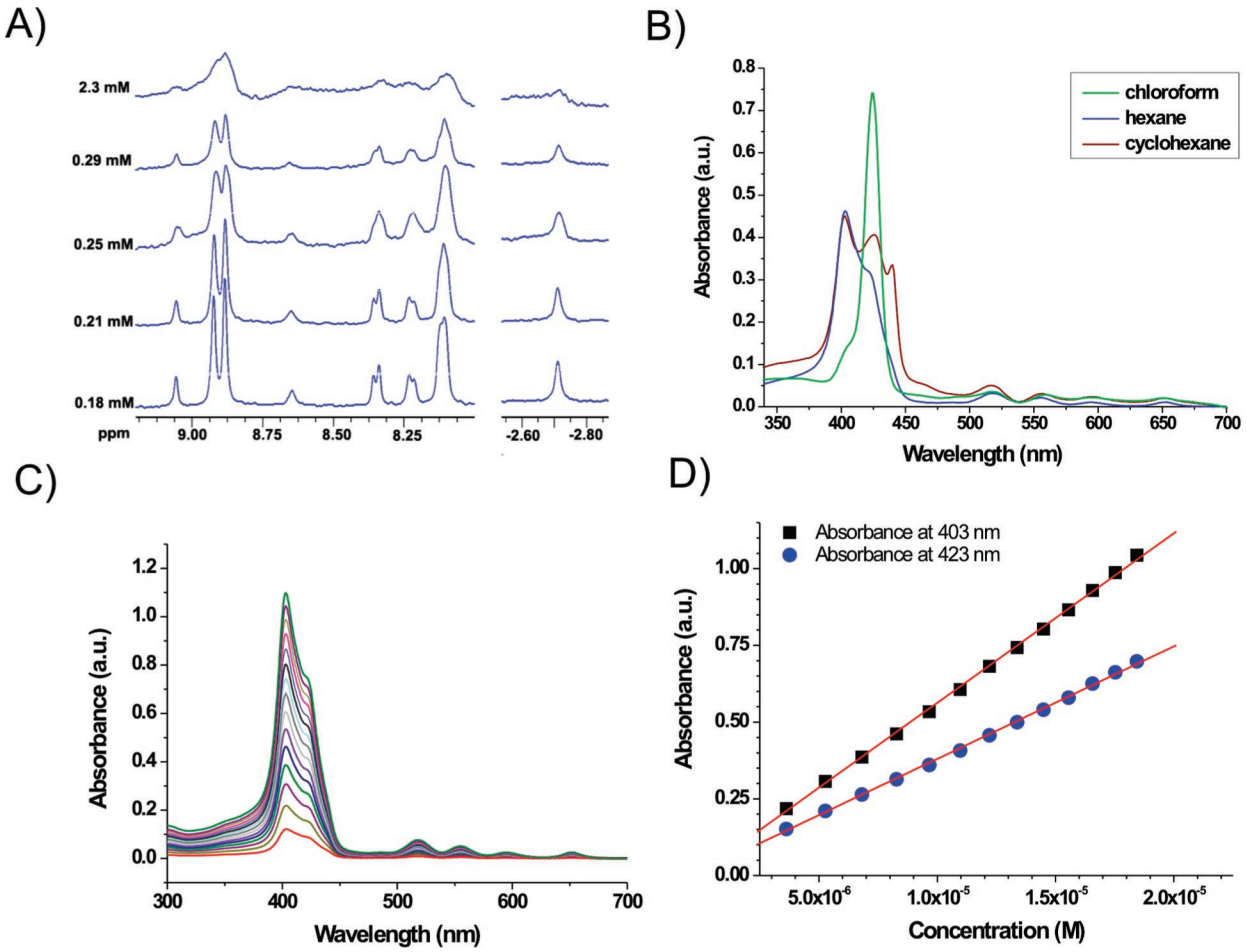

Figure 2. (A) ^{1}H NMR spectra in $CDCl_3$ of the aromatic region and the region of the pyrrole NH protons of **1b** as a function of concentration. (B) UV−vis spectra of **1b** in various solvents ([**1b**] = 8.3×10^{-6} M). (C) UV−vis spectra of **1b** in *n*-hexane as a function of concentration. (D) Plots of the absorbance of **1b** in *n*-hexane at 403 and 423 nm as a function of concentration.

an isosbestic point located at 425 nm (Figure 3C). At higher temperatures no further changes were observed in the spectra. The combined UV−vis and CD data suggest that in *n*-hexane the porphyrins in the stack of **1b** have both face-to-face and head-to-tail arrangements at elevated temperatures, but at ambient temperatures a face-to-face arrangement is more favored.

The CD spectrum of **1b** in cyclohexane deceptively seems to resemble the CD spectrum of this compound in *n*-hexane at elevated temperatures (Figure 3A). Deconvolution of the signals in the former spectrum, however, indicated the presence of three Cotton effects, located at 401, 426, and 443 nm, respectively (see Supporting Information), of which the latter two are opposite of sign compared to the spectrum of **1b** in *n*-hexane at elevated temperatures. All three Cotton effects can be directly correlated with the absorption bands in the UV−vis spectrum of **1b** in cyclohexane and exhibit no significant temperature dependence in the range 6.5−70 °C.

Most importantly, in a solution of **1b** in cyclohexane a signal at 190 nm was observed, originating from the amide functions, which can only be explained by a transfer of chirality from the periphery of the porphyrin trimer to the core (Figure 3B). This observation strongly suggests that **1b** assembles into a helical columnar stack. The presence of strong CD signals, even at elevated temperatures in both cyclohexane and *n*-hexane supports the presence of very stable aggregates of **1b** in these solvents. These results can be interpreted by the tightening and loosening of the helix as a function of temperature. The dominating forces in the helix are intermolecular hydrogen bonding and $\pi-\pi$ stacking. We tentatively propose that, upon warming, the helix loosens, because the $\pi-\pi$ interactions are more sensitive to temperature than the hydrogen bonding, which wants the helix to possess a twist of 60°. The overall structure is a compromise between the two competing forces.

To unambiguously demonstrate the aggregation of **1b**, dynamic and static light scattering measurements were performed. Consistent with the UV−vis and CD measurements, no aggregates were detected in chloroform. Dynamic light scattering demonstrated that in both *n*-hexane and cyclohexane comparable particles were present with a hydrodynamic radius of 28 ± 2 nm (Figure 4A,B).

The static light scattering intensity profiles of the aggregates in both solvents could be fitted by assuming a thin rigid rod, with a length of ca. 300 nm (Figure 4C). In combination with the measured hydrodynamic radius, it is now possible to roughly determine the diameter of the columnar stack,[13] which amounts to 5 ± 1 nm. This value is in good agreement with the diameter of one molecule of

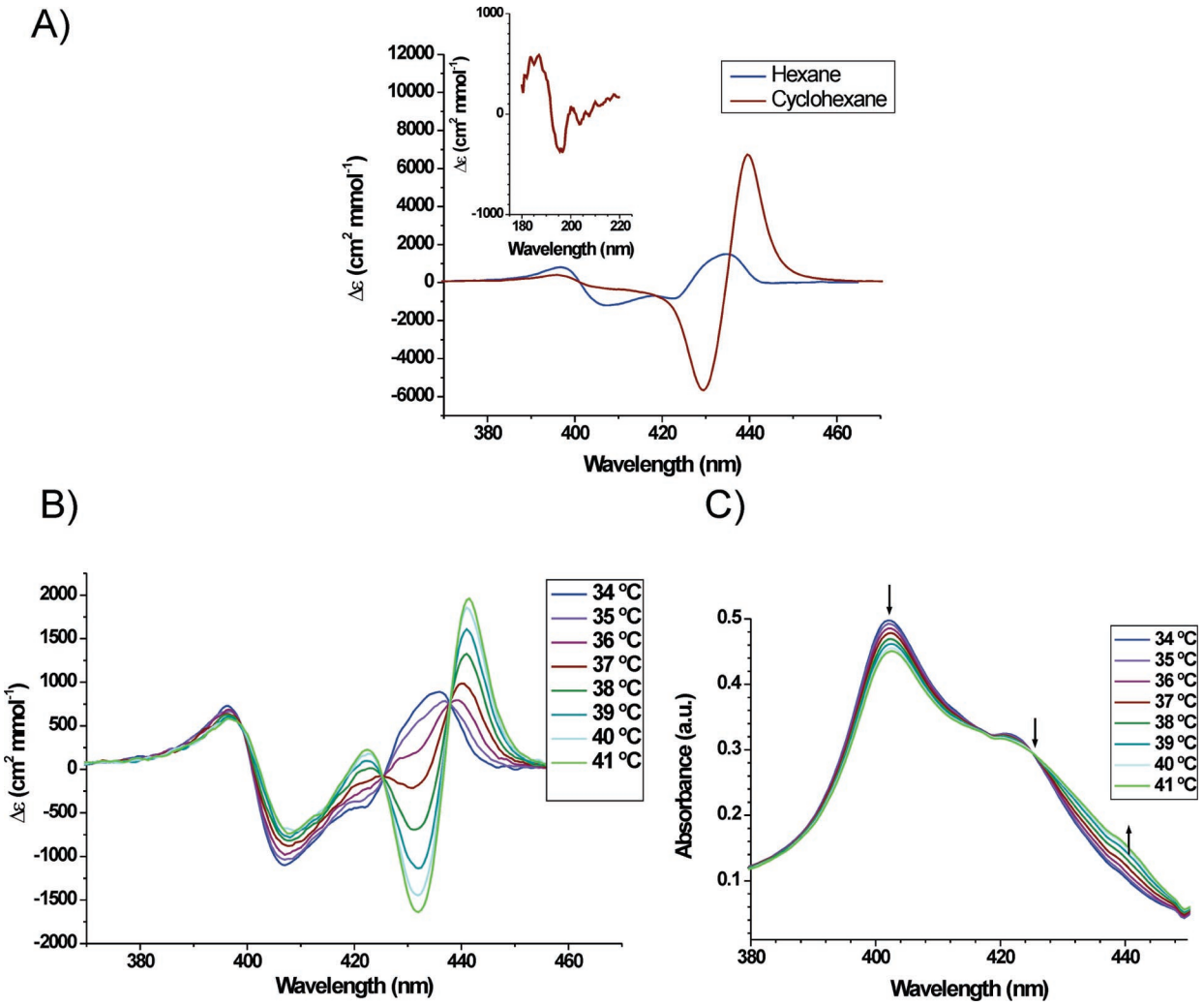

Figure 3. (A) CD spectra of **1b** in *n*-hexane and cyclohexane ([**1b**] = 8.3 × 10^{-6} M, T = 25 °C). Inset: CD signal originating from the amide functions of **1b** in cyclohexane ([**1b**] = 8.3 × 10^{-6} M, T = 25 °C). The absorbance of *n*-hexane in the amide region prevents a reliable CD measurement in this region in this solvent. CD spectra (B) and UV−vis spectra (C) in *n*-hexane as a function of temperature ([**1b**] = 2.9 × 10^{-5} M).

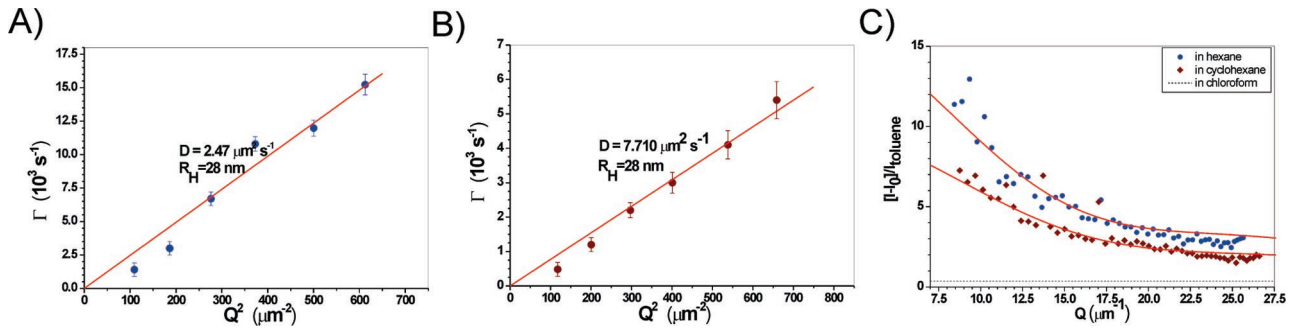

Figure 4. (A) Plot of the decay rate (Γ) as a function of the scattering wavevector squared (Q^2) determined by dynamic light scattering measurements in *n*-hexane ([**1b**] = 3 × 10^{-5} M). (B) Same as for (A) but in cyclohexane. The slopes of the plots yield the translational diffusion coefficient D from which, via the Stokes−Einstein relation, the hydrodynamic radius (R_H) can be determined. (C) Static light scattering intensity profiles in different solvents. In the case of *n*-hexane and cyclohexane, the solid lines are fitted assuming a thin rigid rod with a length of 300 ± 50 nm.

1b, viz. 4.5 nm, and implies that **1b** self-assembles in solution into supramolecular polymers, consisting of stacks which contain on average 500 molecules of **1b** and thus have an average mass of 1.8 million Dalton.

Time-resolved fluorescence anisotropy measurements confirmed the presence of aggregates of **1b** in *n*-hexane and cyclohexane (Figure 5). A strong polarization was found in both *n*-hexane and cyclohexane, but only a slight polarization

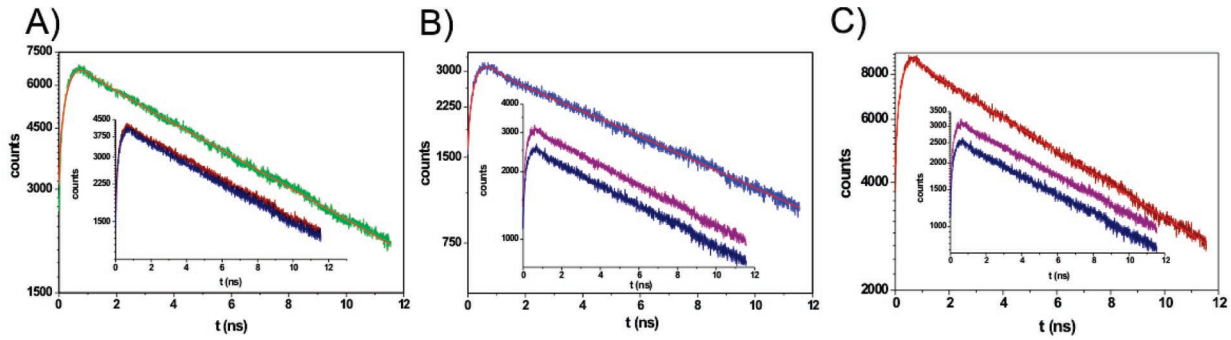

D)

Solvent	A_1	τ_1 (ns)	A_2	τ_2 (ns)	$r_{0\infty}$
chloroform	0.15	1.1	0.85	9.4	0.02
n-hexane	0.45	0.5	0.55	9.6	0.07
cyclohexane	0.7	0.6	0.3	9.5	0.1

Figure 5. Time-resolved fluorescence measurements on **1b** in chloroform (A), *n*-hexane (B), and cyclohexane (C) ([**1b**] = 3×10^{-5} M). In all cases, the fluorescence decay exhibits a biexponential behavior. The inset of each figure reports the VV and VH components of the fluorescence decay curve. (D) Overview of the fluorescence photophysical parameters (relative amplitude (A_i), lifetime (τ_i), and asymptotic anisotropy ($r_{0\infty}$)), determined by fitting of the fluorescence decay plots (red solid curves).

was observed in chloroform (Figure 5D). The lower asymptotic anisotropy value and the longer average fluorescence lifetime in chloroform are in agreement with the presence of single molecules of **1b**. In contrast, the average fluorescence lifetime in *n*-hexane and cyclohexane is much smaller as a result of the assembly of **1b** into columnar stacks. All the experimental evidence highlights that **1b** has a strong preference to form columnar assemblies and that the observed behavior is a result of intermolecular stacking.

In a recent paper we have reported that **1a** spontaneously forms extended domains of periodic patterns upon drop-casting a solution of this compound in chloroform onto a mica surface.[4] These patterns consisted of equidistant parallel lines, built up from extremely long columnar stacks that are one single molecule thick. Besides the propensity of the molecules to self-assemble in 1D aggregates, the pattern formation process and periodicity of the lines were found to be governed by physical dewetting processes, i.e., the "coffee-stain mechanism"[6,19] and spinodal dewetting.[20−23]

When a droplet of a solution of **1b** in chloroform ([**1b**] = 5.7×10^{-6} M, droplet size = 3 μL) was drop-casted onto a mica surface under an argon atmosphere at a temperature of 22 ± 0.5 °C and the solvent was allowed to evaporate, similar domains of highly ordered line patterns were observed, which are oriented parallel to the contact line (Figure 6A). Each line has a height of 4.3 ± 0.4 nm (see Supporting Information), indicating that it consists of a single molecule thick columnar stack of **1b**. Like in the case of **1a**, the periodicity of the patterns formed by **1b** was found to be monodisperse within one domain (e.g., 500 ± 70 nm, see Supporting Information), but between domains the periodicity varied. The domain sizes, as well as the lengths of a single linear assembly of **1b** were reduced compared to the patterns formed by **1a**.

The pattern formation was found to be highly dependent on the concentration of **1b**: only in the concentration range of 1−10 μM were domains with such a periodic pattern observed. At higher concentrations, AFM images typical for gels were obtained, whereas at lower concentrations small droplets composed of randomly deposited material were observed. One of the key features that governs pattern formation is the self-assembly properties of the molecule. The strict concentration dependence suggests that the periodic patterns are only formed if the concentration of **1b** in a thin film, which is subject to spinodal dewetting at a thickness of 10−100 nm, is such that the molecules start to self-assemble (viz. $\sim$ 0.2 mM, vide supra).

Like thin chloroform films, thin *n*-hexane films on flat substrates are subject to spinodal dewetting,[23] but their dewetting properties are expected to be quite different. In addition, in *n*-hexane already at micromolar concentrations aggregates of **1b** are present. When a solution of **1b** in *n*-hexane ([**1b**] = 5.7×10^{-6} M) was drop-casted onto mica and the solvent allowed to evaporate, AFM revealed the presence of very long self-assembled fibers (Figure 6B), with lengths up to several microns and a height of 3.6 ± 0.5 nm (see Supporting Information), which indicates that they still exist of single molecule thick columnar stacks.[24] It is of interest to note that the height of these fibers is somewhat smaller than the height of the lines observed after drop-casting a chloroform solution of **1b**. This difference might be a result of a slightly different packing of the molecules of **1b** in the fibers compared to those in the lines, which is expressed in a different diameter of the resulting stack. Alternatively, the larger diameter of the lines deposited from chloroform might be attributed to a swelling effect, which has also been observed before in AFM studies on rodlike polyisocyanides with peptide side chains that were deposited from the same solvent.[25] In contrast to the defined line patterns deposited from chloroform, the fibers deposited from *n*-hexane are oriented randomly all over the sample and no relation between the orientation of the fibers and the local

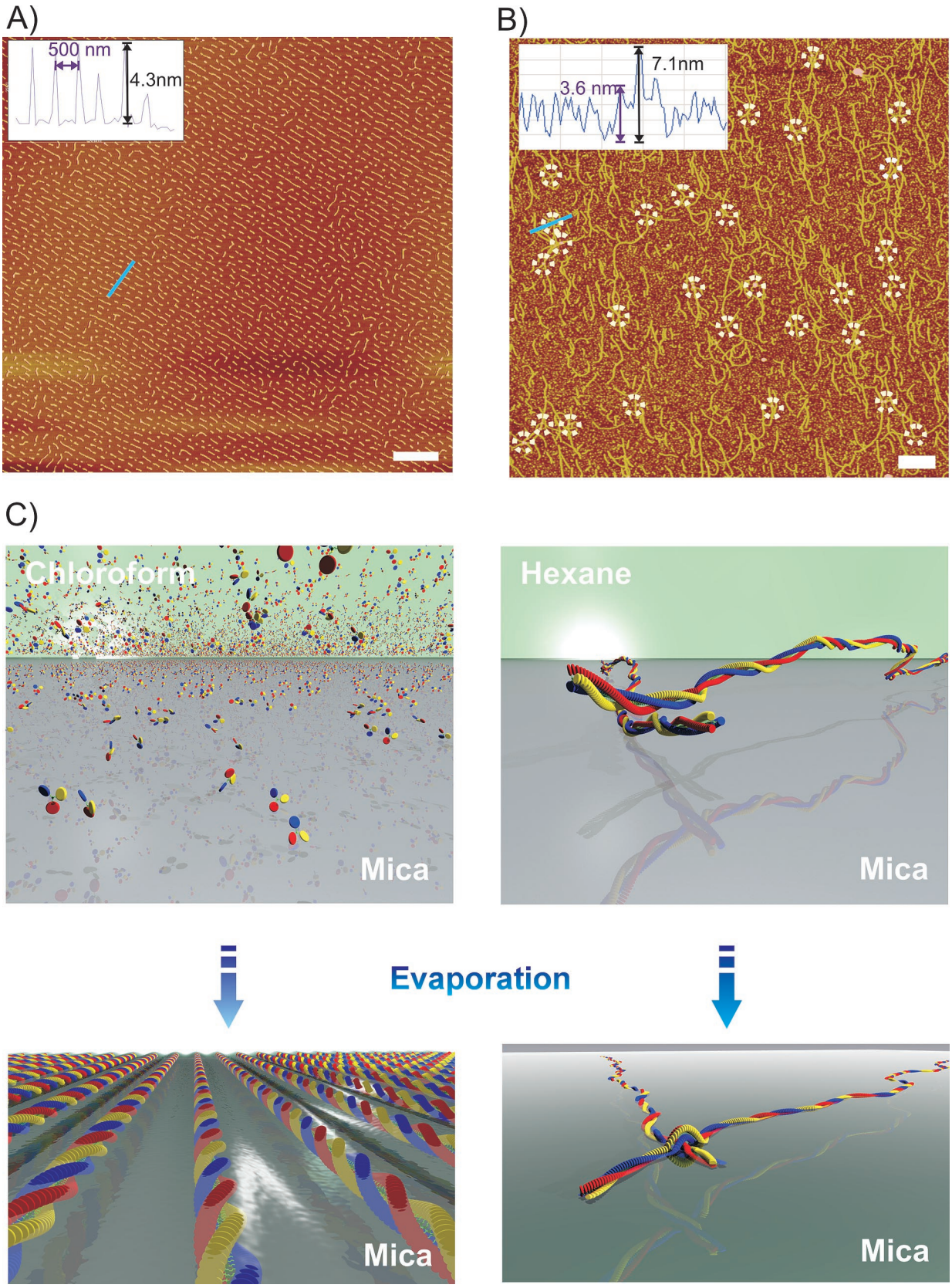

Figure 6. (A,B) AFM images of patterns formed after drop-casting a solution of **1b** in chloroform (A, scale bar = 1 μm) and *n*-hexane (B, scale bar = 2 μm). The dashed circles highlight the crossing points of the fibers. The height of a crossover point measures twice the thickness of a fiber, indicating that these fibers are on top of each other (inset). (C) Artist impression of the aggregation behavior of **1b** in solution and at the solid−liquid interface with chloroform and *n*-hexane as a solvent.

solvent front was observed. The fact that many of the fibers overlapped each other strongly suggests that they are formed in solution and deposited as such onto the mica surface (Figure 6C). The apparent alignment is probably the result

of a flow of the solvent that occurs during the evaporation of the droplet. The fact that the fibers are distributed randomly demonstrates that in the case of *n*-hexane spinodal dewetting does not significantly influence the deposition of the aggregates, which is likely the result of the limited mobility of the large aggregated species in the thin film; i.e., it behaves as a (supramolecular) polymer.[11] The size distribution of the fibers is rather large (Figure 6B). Because of the presence of several very long aggregates, the calculated average length of the fibers is 535 ± 450 nm. The majority of them, however, have a length in the range 100−325 nm (see Supporting Information).

The aggregation behavior of **1b** in *n*-hexane strongly suggests that the periodic patterns formed upon evaporation of a chloroform solution are not composed of preformed columnar stacks of this compound. Instead, they are formed by a highly directional self-assembly process, which is templated by the undulating patterns caused by the spinodal dewetting, that occurs simultaneously.

In conclusion, it is shown that in *n*-hexane and cyclohexane compound **1b** self-assembles already at micromolar concentrations into long chiral supramolecular polymers, which precipitate upon drop-casting a solution of **1b** onto a mica surface. In contrast, in chloroform, **1b** is molecularly dissolved up to concentrations of 0.2 mM. Upon drop-casting micromolar solutions onto mica, supramolecular polymers do not precipitate but are only formed at the moment the chloroform film becomes subject to spinodal dewetting, resulting in the formation of highly periodic line patterns.

Acknowledgment. Supported by grants from The Netherlands Organization of Scientific Research (NWO) to J.A.A.W.E. (VENI grant) and A.E.R. (VIDI grant); the National Research School Combination Catalysis to R.v.H. and to R.J.M.N.; the Royal Netherlands Academy of Science to R.J.M.N.; NanoNed, the Dutch nanotechnology program of the Ministry of Economic Affairs; and the Dutch Foundation for Fundamental Research on Matter (FOM).

Supporting Information Available: Supporting Figure 1 contains the deconvoluted UV−vis spectra of **1b** in *n*-hexane and cyclohexane, and supporting Figure 2 shows the deconvoluted CD-spectra of **1b** in these solvents. Supporting Figure 3 contains the UV−vis and CD spectrum of **1b** in *n*-hexane at an elevated temperature ($T = 41$ °C). Supporting Figures 4 and 5 contain respectively the statistics on the AFM measurements at the chloroform/mica and at the *n*-hexane/mica interface. In addition, the supporting material contains a description of all the experimental details. This material is available free of charge via the Internet at http://pubs.acs.org.

References

(1) Percec, V.; Glodde, M.; Bera, T. K.; Miura, Y.; Shiyanovskaya, I.; Singer, K. D.; Balagurusamy, V. S. K.; Heiney, P. A.; Schnell, I.; Rapp, A.; Spiess, H. W.; Hudson, S. D.; Duan, H. *Nature* **2002**, *419*, 384.
(2) Jacobs, H. O.; Tao, A. R.; Schwartz, A.; Gracias, D. H.; Whitesides, G. M. *Science* **2002**, *296*, 323.
(3) Elemans, J. A. A. W.; van Hameren, R.; Nolte, R. J. M.; Rowan, A. E. *Adv. Mater.* **2006**, *18*, 1251.
(4) van Hameren, R.; Schön, P.; van Buul, A. M.; Hoogboom, J.; Lazarenko, S. V.; Gerritsen, J. W.; Engelkamp, H.; Christianen, P. C. M.; Heus, H. A.; Maan, J. C.; Rasing, T.; Speller, S.; Rowan, A. E.; Elemans, J. A. A. W.; Nolte, R. J. M. *Science* **2006**, *314*, 1433.
(5) Palermo, V.; Samori, P. *Angew. Chem., Int. Ed.* **2007**, *24*, 4428.
(6) Deegan, R. D.; Bakajin, O.; Dupont, T. F.; Huber, G.; Nagel, S. R.; Witten, T. A. *Nature* **1997**, *389*, 827.
(7) Vyawahare, S.; Craig, K. M.; Scherer, A. *Nano Lett.* **2006**, *6*, 271.
(8) Smalyukh, I. I.; Zribi, O. V.; Butler, J. C.; Lavrentovich, O. D.; Wong, G. C. L. *Phys. Rev. Lett.* **2006**, *96*, 177801.
(9) Jeukens, C. R. L. P. N.; Lensen, M. C.; Wijnen, F. J. P.; Elemans, J. A. A. W.; Christianen, P. C. M.; Rowan, A. E.; Gerritsen, J. W.; Nolte, R. J. M.; Maan, J. C. *Nano Lett.* **2004**, *4*, 1401.
(10) Huang, J.; Kim, F.; Tao, A. R.; Connor, S.; Yang, P. *Nat. Mater.* **2005**, *4*, 896.
(11) van Herrikhuyzen, J.; Schenning, A. P. H. J.; Jonkheijm, P.; Meijer, E. W. *Org. Biomol. Chem.* **2006**, *4*, 1539.
(12) Jonkheijm, P.; van der Schoot, P.; Schenning, A. P. H. J.; Meijer, E. W. *Science* **2006**, *313*, 80.
(13) Micali, N.; Villari, V.; Castriciano, M. A.; Romeo, A.; Monsù Scolaro, L. *J. Phys. Chem. B.* **2006**, *110*, 8289.
(14) Wilson, A. J.; Masuda, M.; Sijbesma, R. P.; Meijer, E. W. *Angew. Chem., Int. Ed.* **2005**, *44*, 2275.
(15) Hirschberg, J. H. K. K.; Brunsveld, L.; Ramzi, A.; Vekemans, J. A. J. M.; Sijbesma, R. P.; Meijer, E. W. *Nature* **2000**, *407*, 167.
(16) Brunsveld, L.; Prince, R. B.; Meijer, E. W.; Moore, J. S. *Org. Lett.* **2000**, *2*, 1525.
(17) Kasha, M.; Rawls, H. R.; Ashraf El-Bayoumi, M. *Pure Appl. Chem.* **1965**, *11*, 371.
(18) Hunter, C. A.; Sanders, J. K. M. *J. Am. Chem. Soc.* **1990**, *112*, 5525.
(19) Deegan, R. D. *Phys. Rev. E* **2000**, *61*, 475.
(20) Sferrazza, M.; Heppenstall-Butler, M.; Cubitt, R.; Jones, R. A. L. *Phys. Rev. Lett.* **1998**, *81*, 5173.
(21) Higgins, A. M.; Jones, R. A. L. *Nature* **2000**, *404*, 476.
(22) Sharma, A.; Khanna, R. *Phys. Rev. Lett.* **1998**, *81*, 3463.
(23) Moriarty, P.; Taylor, M. D. R.; Brust, M. *Phys. Rev. Lett.* **2002**, *89*, 248303.
(24) Stocker, W.; Beckmann, J.; Stadler, R.; Rabe, J. P. *Macromolecules* **1996**, *29*, 7502.
(25) Zhuang, W.; Ecker, C.; Metselaar, G. A.; Rowan, A. E.; Nolte, R. J. M.; Samori, P.; Rabe, J. P. *Macromolecules* **2005**, *38*, 473.

NL072563F